SF2A 2012
S. Boissier, P. de Laverny, N. Nardetto, R. Samadi, D. Valls-Gabaud and H. Wozniak (eds)

CHARACTERISING EXOPLANET ATMOSPHERES WITH ECHO: UPDATED RESULTS FOR A NEW PAYLOAD DESIGN

M. Tessenyi[1], J.-P. Beaulieu[1, 2], M. Ollivier[3], G. Tinetti[1], V. Coudé du Foresto[4] and J.-M. Reess [4]

Abstract. The field of exoplanets is one of the fastest growing and most novel in astrophysics, with hundreds of planetary discoveries and thousands of candidates waiting to be confirmed. Many of these planets are very different from the planets in our Solar System, yet at present we do not have an explanation nor a clear understanding of this diversity. The atmospheric composition of these remote worlds may provide a key to interpreting this diversity. Spectroscopic measurement of transiting exoplanets is the only viable technique we can use today to sound these exotic atmospheres. EChO, the Exoplanet Characterization Observatory is a Medium class ESA mission candidate, currently being assessed as part of the COSMIC VISION programme. EChO will be the first mission fully dedicated to the systematic study of the physics and chemistry of a large portfolio of exoplanet atmospheres. The targets will cover a wide range of planets: from hot planets to temperate ones, from large, gaseous Jupiter-like planets to small telluric planets. The baseline mission design is a 1.2 m off axis telescope with one instrument composed of several channels covering the spectral range 0.4-16 μm with a spectral resolution in the 300-30 range. The satellite is optimised for stability and is based on the legacy of previous successful ESA missions. EChO will observe primary transits and secondary eclipses, and also phase curves of some non-transiting planets. We present updated results for secondary eclipses, based on methods from previous studies and incorporating the evolution of the payload design.

Keywords: exoplanets, atmospheres, EChO, stars

1 The EChO Instrument

The Exoplanet Characterisation Observatory (EChO) is a proposed 1.2 m space-based telescope currently under study at the European Space Agency, as a M class mission part of the Cosmic Vision programme (Tinetti et al. 2012, `sci.esa.int/echo/`). EChO will provide simultaneous, multi-wavelength spectroscopic observations on a stable platform for a wide selection of exoplanets, from the visible to the mid-infrared. The science case of EChO is described in Tinetti et al. (2011). In Tessenyi et al. (2012) we have studied the feasibility and general performance of an EChO like mission for a broad selection of targets. In that paper, we considered a number of instrument tradeoffs, which included two telescope sizes and several possible choices for the detector technology. In this study, we focus on the performances of our most recent payload design, studied during the assessment phase by our instrument consortium (Swinyard et al. 2012, Reess et al., 2012, Adriani et al. 2012, Focardi et al. 2012, Pascale et al. 2012, Eccleston et al. 2012, Ramos Zapata et al. 2012). The updated instrument design consists of a 1.2 m telescope and detector settings which are listed in Table 1. Further studies will include results from EChOSIM, an end-to-end instrument simulator currently under development by our instrument consortium.

[1] University College of London, Gower Street, London, United Kingdom
[2] Institut d'Astrophysique de Paris, CNRS, UMPC, 98bis Boulevard Arago, 75014 Paris, France
[3] IAS - UPS - CNRS, Bat 120, 91405 Orsay, France
[4] LESIA, Observatoire de Paris, Meudon, 5 Place Jansen, 92190 Meudon, France

Table 1. Instrument settings used in our simulations, listed for each observing band used. In addition, the two following settings are the same for all four bands considered: a 30 μm pixel size and 4 illuminated pixels per spectral element are assumed.

Instrument Values	Visible	2.5 to 5 μm	5 - 11 μm	11 to 16 μm
Detector used	MCT	MCT	Si:As	Si:As
Full well capacity (electrons)	$2 \cdot 10^6$	$4 \cdot 10^6$	$2 \cdot 10^5$	$2 \cdot 10^5$
Dark current (electrons/s/pixel)	0.1	10	0.2	0.2
Quantum efficiency (electrons/photon)	0.5	0.7	0.7	0.7
Readout noise (electrons/pixel/readout)	10	400	15	15
Readout time (seconds)	0.004	0.01	3	3
Telescope temperature (K)	-	60	60	60
Instrument temperature (K)	-	45	45	45
Detector temperature (K)	170	< 45	7	7
Telescope transmission	0.86	0.86	0.86	0.86
Instrument transmission	0.7	0.32	0.35	0.35

2 Planets considered

In Tessenyi et al. (2012) a wide variety of target cases are considered, here the focus is on four key cases: a Hot Jupiter and Warm Neptune as examples of gaseous planets (HD 189733b and GJ 436b, respectively), and a Hot super-Earth and temperate super-Earth (Cnc 55 e and a possible 1.8 $R_\oplus$, 5 $M_\oplus$ super-Earth in the habitable-zone of a M dwarf). The parameters assumed for these targets are listed in Table 2. Where possible, the spectra of the planets presented are modelled atmospheres, and blackbody curves are used when no observational data is available. Figure 1 shows the planet/star flux ratio (contrast) of the Hot Jupiter and the Warm Neptune, which were obtained using radiative transfer codes as described in Tessenyi et al. (2012). These simulations either fit existing observations (e.g., Knutson et al. 2007, Tinetti et al., 2007b, Charbonneau et al., 2008, Grillmair et al., 2008, Swain et al., 2008, Stevenson et al. 2010, Beaulieu et al., 2011) or are an extrapolation from our knowledge of Solar System planets. Figure 2 shows the contrast values used for the Hot and Temperate super-Earths. For the Hot super-Earth case, the planet temperature is expected to be between 1980 and 2800 K, depending on the heat redistribution on the planet (Winn et al. 2011). For the integration time calculations, a mean temperature of 2390 K is used. For the Temperate super-Earth three possible atmospheres are presented: an Earth-like, Venus-like and a Small Neptune-like spectrum, reflecting the effect of atmosphere compositions on the emitted signal. An average temperature of 300 K, fitting within the temperature range of the atmosphere types, is used as planet/star flux ratio. These Temperate super-Earths will be the most challenging targets to observe, with flux ratios in the $10^{-5} - 10^{-4}$ range, and will require low resolution observations. The spectra presented for this target in Figure 2 are set at R=20.

Table 2. Star and planet parameters assumed for the selected targets of this study. The planet radii are given both in units of Jupiter radius and Earth radius, and the temperatures listed are an average temperature from the temperature-pressure profile.

Star	Hot Jupiter	Warm Neptune	Hot super-Earth	Temperate super-Earth
Spectral Type	K1V	M2.5V	G8V	M4.5V
Radius ($R_\odot$)	0.8	0.464	0.95	0.22
Mass ($M_\odot$)	0.8	0.452	0.91	0.22
Temperature (K)	4980	3684	5196	3300
Planet				
Radius (R_{jup} | $R_\oplus$)	1.138 | 12.77	0.365 | 4.10	0.194 | 2.18	0.16 | 1.8
Temperature (K)	1350	750	2390	250
Semi-major axis (au)	0.031	0.029	0.016	0.046
Period (days)	2.219	2.644	0.737	7.64
Transit duration (hr)	1.83	1.03	1.76	1.39

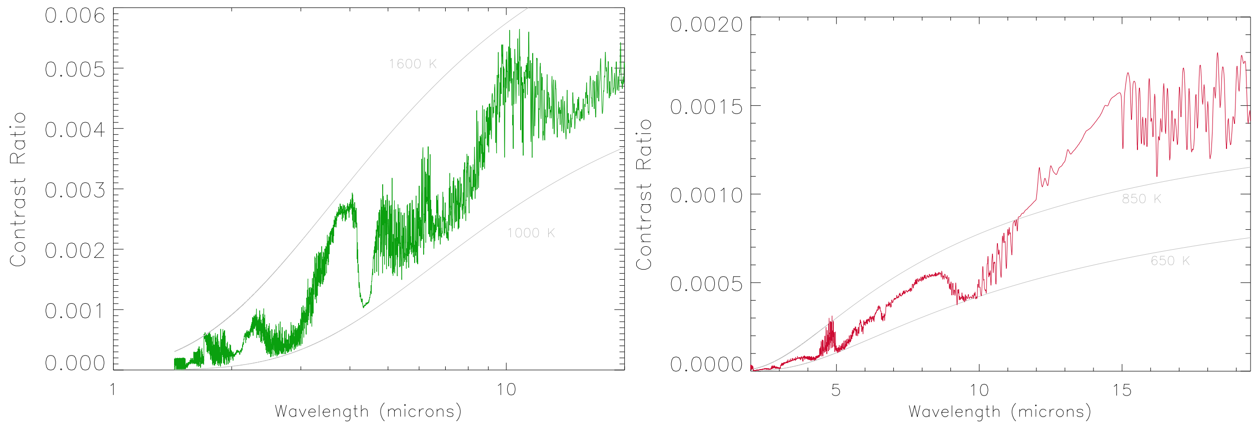

Fig. 1. Left: Modeled emission spectrum of HD 189733b (Tessenyi et al., 2012), a hot-Jupiter around a K1/2V star, mag. V=7.67, presented as planet/star flux ratio. Blackbody curves at 1000 K and 1600 K are plotted in grey for indication. **Right:** Modeled planet/star flux ratio of GJ 436b (Tessenyi et al., 2012), a warm Neptune orbiting a M2.5V star, with 650 K and 850 K blackbody curves plotted for indication.

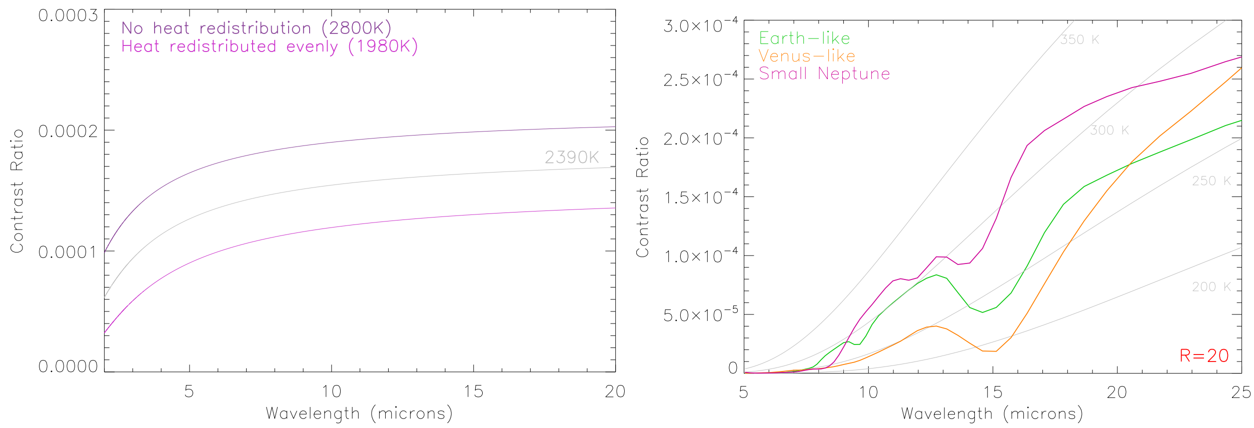

Fig. 2. Left: Blackbody planet/star flux ratio for Cnc 55 e, a 2.1 $R_{\oplus}$ Hot super-Earth, orbiting a G8V star. The planet temperature is estimated to be between the 2800 K and 1980 K limits, depending on the heat redistribution in the atmosphere (Winn et al. 2011). A mean temperature of 2390 is used for this study. **Right:** Low resolution (R=20) Earth-like, Venus-like and Small Neptune-like planet/star flux ratio for a possible 1.8 $R_{\oplus}$ Temperate super-Earth, orbiting a 3150 K M4.5V star. The three spectra show possible atmospheric types that could exist in this temperature regime. An average temperature of T=300 K is used for our calculations.

3 Updated results

The results are given as integration times in number of transits required (integration time divided by the transit duration) in Tables 3 and 4. The computed contrast value is sampled at three different wavelengths: 3, 7.5 and 13.5 μm, for a wavelength bin corresponding to a single resolution element of the channel (resolving power 300, 30 and 30 for the three channels, respectively). The integration time is computed in the bins for a range of stellar magnitudes, either in V mag of K mag, with the given contrast and a desired signal-to-noise ratio (SNR) value. A minimum SNR=5 setting is used for all targets, and where the signal permits, higher SNR integration times are presented. Table 3 shows the results for the Hot Jupiter and the Warm Neptune cases, and Table 4 presents the results for the Hot and Temperate super-Earths.

Table 3. **Top:** Hot Jupiter integration times (in units of "number of transits") needed to obtain the specified SNR (5 and 50) per channel for a given brightness (in Mag. V), with a 0.8 $R_{\odot}$, K1V star at 4980 K. For the SNR=5 requirement this planet case is easy to observe. The SNR=50 requirement requires adding up of observations, mostly due to the higher resolution required in the first channel. Within the proposed 5 year mission lifetime, this planet will complete 826 orbits. **Bottom:** Integration times (in units of "number of transits") for a Warm Neptune, orbiting a M2.5V star at 3150 K. Results are given per channel for two SNR cases (5 and 25) and a given brightness (in Mag. K). For this target, in the 1-5 μm channel, binning of the signal to a lower resolution will be required to obtain enough photons, as the contrast is low in this band. In 5 years this planet will complete 691 orbits.

Hot Jupiter – Secondary eclipse, SNR=5

Channel range	λ (μm)	Res. Power	Contrast ($*10^{-3}$)	Integration time (n. transits) V=5	V=6	V=7	V=8	V=9
1-5	3	300	0.40	0.1	0.2	0.5	1.4	3.5
5-11	7.5	30	2.77	< 0.1				
11-16	13.5	30	3.93	< 0.1				

Secondary eclipse, SNR=50

Integration time (n. transits) V=5	V=6	V=7	V=8	V=9
9	22	55	138	348
0.3	0.3	0.5	1.2	3
0.2	0.4	1	2.5	7

Warm Neptune – Secondary eclipse, SNR=5

Channel range	λ (μm)	Res. Power	Contrast ($*10^{-3}$)	Integration time (n. transits) K=5	K=6	K=7	K=8	K=9
1-5	3	300	0.02	351	*Lower Resolution*			
5-11	7.5	30	0.45	0.3	0.7	1.9	5	12
11-16	13.5	30	1.28	0.2	0.4	1.1	3.2	11

Secondary eclipse, SNR=25

Integration time (n. transits) K=5	K=6	K=7	K=8	K=9
Lower Resolution				
8	19	47	117	293
3.8	10	27	80	277

4 Conclusions

We have presented updated results of our previous work estimating the performance of EChO, building on the evolution of the instrument design. We have shown that with a 1.2 m space-based telescope and an updated payload design, key cases of transiting exoplanets can be observed spectroscopically from the visible to the mid-infrared, with a choice of SNR/resolution observation modes. These updated results confirm the strengths of EChO: a wide range of planet types can be observed within 5 years, with the flexibility of observing bright targets either at high accuracy or repeatedly at lower SNR and resolution. The repeated observation of bright targets will allow the study of atmospheric circulations, or the "slicing" of planet observations to map the planet surface during ingress and egress, maximising the science return of the mission. Challenging targets such as Temperate super-Earths can be observed with lower SNR/resolution, provided they orbit close-by and late type M dwarfs. Overall, EChO will provide full emission (and transmission) spectra from the visible to the mid-infrared for a wide variety of targets, contributing to the advancement of this new, exciting field.

References

Adriani A., Oliva E., Piccioni G., et al. 2012, Proc. SPIE 8442, 84422W

Beaulieu J.P., Tinetti G., Kipping D. et al. 2011, ApJ, 731, 16

Charbonneau D., Knutson H. A., Barman T., et al., 2008, ApJ, 686, 1341

Table 4. Top: Hot super-Earth integration times (in units of "number of transits") needed to obtain the specified SNR (5 and 25) per channel for a given brightness (in Mag. V), with a 0.95 $R_\odot$, G8V star at 5196 K. As the Hot Jupiter, with the SNR=5 requirement this planet case is easy to observe. The SNR=25 requirement requires adding up of observations, mostly due to the higher resolution required in the first channel. Within the proposed 5 year mission lifetime, this planet will complete 2467 orbits. **Below:** Integration times (in units of "number of transits") for a Temperate super-Earth, orbiting a M4.5V star at 3300 K. Results are given per channel with an SNR=5, resolution of 10 and a given brightness (in Mag. K). For this target the 1-5 μm channel is not used as a 300 K blackbody object will emit no radiation below $\sim$ 5 μm. Given the lower contrast values for this target, only the SNR=5 case is considered, and for the more distant stars, photometry may be required to observe a target. In 5 years this planet will complete 239 orbits.

Hot super-Earth – Secondary eclipse, SNR=5

Channel range	λ (μm)	Res. Power	Contrast ($*10^{-4}$)	Integration time (n. transits)				
				V=5	V=6	V=7	V=8	V=9
1-5	3	300	0.94	2	4.9	13	31	78
5-11	7.5	30	1.45	1	1	2.2	6	14
11-16	13.5	30	1.62	1.1	2.8	7	19	51

Secondary eclipse, SNR=25

Integration time (n. transits)				
V=5	V=6	V=7	V=8	V=9
49	122	307	771	1944
26	26	54	135	339
28	69	176	460	1268

Temperate super-Earth – Secondary eclipse, SNR=5

Channel range	λ (μm)	Res. Power	Contrast ($*10^{-4}$)	Integration time (n. transits)				
				K=5	K=6	K=7	K=8	K=9
5-11	7.5	10	0.13	159	214	*Photometry*		
11-16	13.5	10	1.06	6	14	39	115	*Ph.*

Eccleston P., Bradshaw T., Coker J., et al. 2012, Proc. SPIE 8442, 84422U-1
Focardi M., Pancrazzi M., Di Giorgio A. M., et al. 2012, Proc. SPIE 8442, 84422T
Grillmair C. J., Burrows A., Charbonneau D., et al. 2008, Nature, 456, 767
Knutson H. A., Charbonneau D., Allen L. E., et al. 2007, Nature, 447, 183
Pascale E., Forder S., Knowles P., et al. 2012, Proc. SPIE 8442, 84422Z
Ramos Zapata G., Belenguer T., Balado A., et al. 2012, Proc. SPIE 8442, 84422V
Reess J.M., Tinetti G., Baier N., et al., 2012, Proc. SPIE 8442, 84421I-1
Stevenson K. B., Harrington J., Nymeyer S., et al. 2010,
Swain M.R., Vasish G., & Tinetti G., 2008, Nature, 452, 329
Swinyard B., Tinetti G., Eccleston P., et al. 2012, Proc. SPIE 8442, 84421G
Tessenyi M., Ollivier M., Tinetti G., et al. 2012, ApJ, 746, 45
Tinetti G., Vidal-Madjar A., Liang M.C., et al., 2007b, Nature, 448, 169
Tinetti G., Cho J. Y.-K., Griffith C. A., et al. 2011, IAU Symposium, 276, 359
Tinetti G., Beaulieu J.P., Henning T. et al. 2012, Experimental Astronomy, 34, 311
Winn J., Matthews J.M., Dawson R.I., et al. 2011, ApJ, 737, L18